

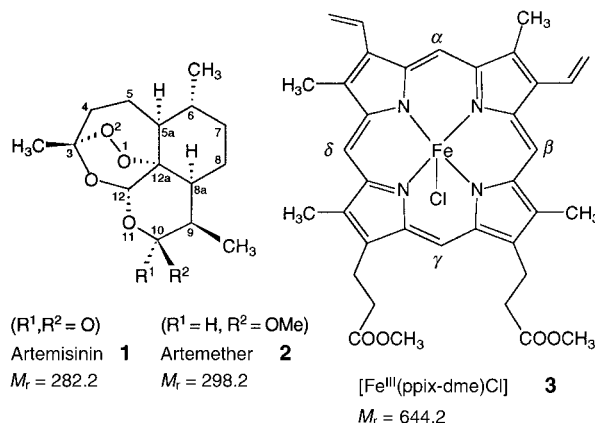
riding atoms. Crystal data for **4**:  $C_{56}H_{68}OsP_2Si_4 \cdot C_6H_6$ ,  $M_r = 1183.71$ ; triclinic, space group  $P\bar{1}$ ;  $a = 12.5486(16)$ ,  $b = 13.5107(18)$ ,  $c = 20.905(3)$  Å,  $\alpha = 90.187(3)$ ,  $\beta = 104.815(3)$ ,  $\gamma = 116.824(2)^\circ$ ,  $V = 3028.7(7)$  Å<sup>3</sup>;  $Z = 2$ ,  $\rho_{\text{calcd}} = 1.298$  g cm<sup>-3</sup>; 20 888 reflections, 13 820 independent reflections ( $R_{\text{int}} = 0.0454$ );  $R_1 = 0.0502$ ,  $wR_2 = 0.0736$  for 630 parameters and 8304 reflections with  $I > 2\sigma(I)$ . The two protons H2A and H12A attached to the vinyl carbon atoms were located in the difference Fourier maps and refined isotropically. Crystal data for **5**:  $C_{48}H_{52}Cl_2OsP_2Si_2$ ,  $M_r = 1008.12$ ; monoclinic, space group  $P2_1/n$ ;  $a = 12.7613(4)$ ,  $b = 17.4260(6)$ ,  $c = 21.4826(7)$  Å,  $\beta = 104.1100(10)^\circ$ ,  $V = 4633.1(3)$  Å<sup>3</sup>;  $Z = 4$ ,  $\rho_{\text{calcd}} = 1.445$  g cm<sup>-3</sup>; 30 794 reflections, 11 178 independent reflections ( $R_{\text{int}} = 0.0478$ );  $R_1 = 0.0327$ ,  $wR_2 = 0.0566$  for 512 parameters and 7697 reflections with  $I > 2\sigma(I)$ . The protons attached to C5 and C6 were located from the difference Fourier maps and refined with isotropic thermal parameters. Crystallographic data (excluding structure factors) for the structures reported in this paper have been deposited with the Cambridge Crystallographic Data Centre as supplementary publication no. CCDC-155319 (**4**) and CCDC-155320 (**5**). Copies of the data can be obtained free of charge on application to CCDC, 12 Union Road, Cambridge CB2 1EZ, UK (fax: (+44) 1223-336-033; e-mail: deposit@ccdc.cam.ac.uk).

- [5] T. B. Wen, S. Y. Yang, Z. Y. Zhou, Z. Lin, C. P. Lau, G. Jia, *Organometallics* **2000**, *19*, 3757.
- [6] H. Werner, S. Jung, B. Webernörfer, J. Wolf, *Eur. J. Inorg. Chem.* **1999**, 951.
- [7] See, for example, a) C. Bianchini, A. Marchi, L. Marvelli, M. Peruzzini, A. Romerosa, R. Rossi, *Organometallics* **1996**, *15*, 3804; b) M. L. Buil, O. Eisenstein, M. A. Esteruelas, C. García-Yebra, E. Gutiérrez-Puebla, M. Oliván, E. Oñate, N. Ruiz, M. A. Tajada, *Organometallics* **1999**, *18*, 4949; c) Y. Kawata, M. Sato, *Organometallics* **1997**, *16*, 1093.
- [8] M. A. Esteruelas, M. Oliván, E. Oñate, N. Ruiz, M. A. Tajada, *Organometallics* **1999**, *18*, 2953.
- [9] a) D. Huang, M. Oliván, J. C. Huffman, O. Eisenstein, K. G. Caulton, *Organometallics* **1998**, *17*, 4700; b) B. Weber, P. Steinert, B. Windmüller, J. Wolf, H. Werner, *J. Chem. Soc. Chem. Commun.* **1994**, 2595; c) L. J. Baker, C. E. F. Rickard, W. R. Roper, S. D. Woodgate, L. J. Wright, *J. Organomet. Chem.* **1998**, *565*, 153.
- [10] a) C. Bohanna, B. Callejas, A. J. Edwards, M. A. Esteruelas, F. J. Lahoz, L. A. Oro, N. Ruiz, C. Valero, *Organometallics* **1998**, *17*, 373; b) H. Werner, M. A. Esteruelas, H. Otto, *Organometallics* **1986**, *5*, 2295.
- [11] a) H. Werner, W. Stüer, N. Laubender, C. Lahmann, R. Herbst-Irmer, *Organometallics* **1997**, *16*, 2236; b) M. A. Esteruelas, F. J. Lahoz, E. Oñate, L. A. Oro, C. Valero, B. Zeier, *J. Am. Chem. Soc.* **1995**, *117*, 7935.
- [12] For recent work on benzynes in organic/organometallic synthesis, see a) E. Yoshikawa, K. V. Radhakrishnan, Y. Yamamoto, *J. Am. Chem. Soc.* **2000**, *122*, 7280; b) M. A. Bennett, C. J. Cobley, A. D. Rae, E. Wenger, A. C. Willis, *Organometallics* **2000**, *19*, 1533; c) S. Tripathy, R. LeBlanc, T. Durst, *Org. Lett.* **1999**, *1*, 1973; d) T. Kitamura, M. Yamane, K. Inoue, M. Todaka, N. Fukatsu, Z. Meng, Y. Fujiwara, *J. Am. Chem. Soc.* **1999**, *121*, 11 674; e) M. Frid, D. Pérez, A. J. Peat, S. L. Buchwald, *J. Am. Chem. Soc.* **1999**, *121*, 9469.
- [13] Y. Wakatsuki, N. Koga, H. Yamazaki, K. Morokuma, *J. Am. Chem. Soc.* **1994**, *116*, 8105.

## Characterization of the Alkylation Product of Heme by the Antimalarial Drug Artemisinin\*\*

Anne Robert, Jérôme Cazelles, and Bernard Meunier\*

Artemisinin **1** and its hemi-synthetic derivatives such as artemether **2** are increasingly used to treat *Plasmodium falciparum* drug-resistant malaria, which causes between one and three million deaths annually.<sup>[1]</sup> The stable endoperoxide bridge of these compounds is required for their antimalarial



activity. The activity of artemisinin is dependent on the cleavage of the endoperoxide by intraparasitic heme, which is generated by the digestion of hemoglobin within infected red blood cells.<sup>[2–5]</sup> In fact, the reductive activation by  $Fe^{II}$ –heme results in the homolytic cleavage of the endoperoxide bond and the subsequent formation of drug-derived carbon-centered radicals, which act as alkylating agents toward either heme or vital parasite proteins. The alkylation of proteins<sup>[6]</sup> or heme<sup>[7]</sup> was observed after the incubation of parasites with pharmacologically relevant concentrations of artemisinin derivatives but no heme–artemisinin or protein–artemisinin adducts had been characterized up to now. Herein we report the first characterized adduct produced by the alkylation of heme by the antimalarial artemisinin.

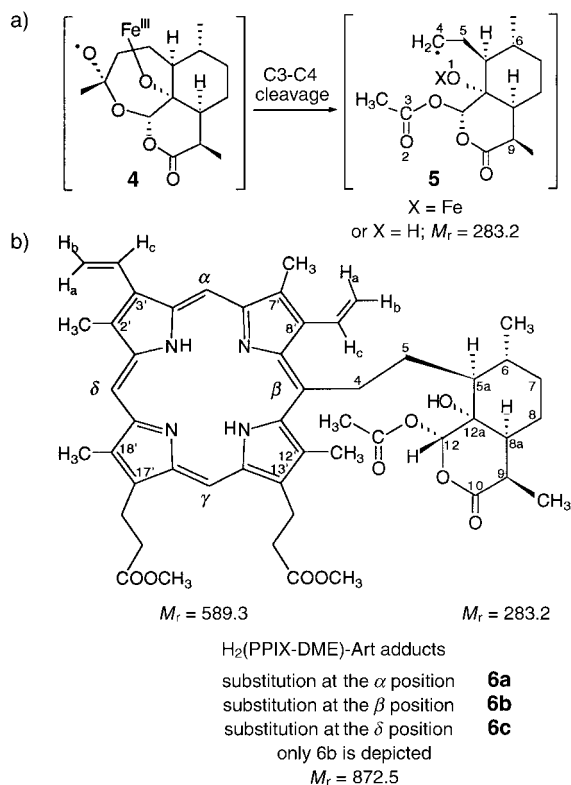
The alkylation of a synthetic metalloporphyrin heme model, manganese(II) tetraphenylporphyrin, by artemisinin,<sup>[8]</sup> artemether, and other synthetic pharmacologically active trioxanes<sup>[9]</sup> has been reported in recent years. Herein, the “true” target of artemisinin, heme, was used. Artemisinin was incubated under an argon atmosphere with the dimethyl ester of hemin, [ $Fe^{III}(ppix-dme)Cl$ ] (**3**), in dichloromethane in the presence of 2,3-dimethylhydroquinone to reduce hemin to

[\*] Dr. B. Meunier, Dr. A. Robert, Dr. J. Cazelles  
Laboratoire de Chimie de Coordination du CNRS  
205 route de Narbonne, 31077 Toulouse cedex 4 (France)  
Fax: (+33) 5-61-55-30-03  
E-mail: bmeunier@lcc-toulouse.fr

[\*\*] We are grateful to the CNRS for financial support, and to the French Ministry of Education for a PhD grant to J.C. Dr. Yannick Coppel (LCC-CNRS) is gratefully acknowledged for discussions on NMR data.

Supporting information for this article is available on the WWW under <http://www.angewandte.com> or from the author.

[Fe<sup>II</sup>(ppix-dme)]. We used the dimethyl ester of heme so that both the drug and the target could be dissolved in one solvent (artemisinin is insoluble in water or in aqueous mixtures). The reductive activation of artemisinin by iron(II)–heme by means of an inner-sphere process resulted in the homolytic cleavage of the peroxide bond to give the oxygen-centered radical **4** (Scheme 1a), as previously observed with the heme model



Scheme 1. Structure of the major artemisinin–heme adducts after demetallation: three regioisomers corresponding to substitution on  $\alpha$ -carbon **6a** (●),  $\beta$ -carbon **6b** (▲),  $\delta$ -carbon **6c** (\*). Only **6b** is depicted. Radical intermediates **4** and **5** result from the heme activation of artemisinin.

manganese(II) tetraphenylporphyrin. This radical promptly rearranged to the sterically unhindered carbon-centered radical **5** by the homolysis of the C3–C4 bond.<sup>[8, 9]</sup> Such a reaction pathway that involves a carbon-centered radical at C4 is important for the antimalarial activity of artemisinin.<sup>[10]</sup> The carbon-centered radical **5**, generated above the plane of the heme derivative, is able to alkylate the macrocycle and produce isomeric covalent adducts. After the reaction of heme with artemisinin for 20–30 min, the conversion of heme was 85–90%, and two new broad peaks were detected (HPLC; 1:1). These peaks correspond to at least two porphyrin derivatives, which gave rise to an intense peak in the ESI-MS at  $m/z = 926.5$  [ $M^+$ ] (the sum of the masses of [Fe<sup>III</sup>(ppix-dme)] ( $M_r = 644.2$ ) and artemisinin fragment **5** (Scheme 1a) after hydrolysis of the oxygen–iron bond ( $M_r = 283.2$ ) minus one mass unit). This result clearly indicates that one hydrogen atom of the metalloporphyrin has been substituted by the artemisinin fragment, **5**, leading to metalated covalent adducts (calculated mass: 926.4) in which both the artemisinin and the heme fragments are present.

To allow a complete characterization of these modified heme residues by NMR spectroscopy, the macrocycle was demetallated *in situ* by using 17 equivalents of Fe<sup>II</sup>SO<sub>4</sub> · 1.5 H<sub>2</sub>O in HCl/CH<sub>3</sub>COOH.<sup>[11]</sup> After purification by column chromatography, the porphyrin–drug material was recovered in 80–85% yield without extensive degradation of the macrocycle. TLC analysis, MS, and NMR spectroscopic data suggested a mixture of sets of heme–drug adducts corresponding to the alkylation of the *meso* positions by the C4-centered artemisinin radical with or without modification of the lactone ring of artemisinin. The heme–drug adducts were fully characterized by MS and NMR spectroscopic analysis of the material containing the unmodified lactone ring (yield: 30–50% depending on the demetallation conditions). This demetallated material was a mixture of three isomers with the same mass of  $m/z = 873.5$  [ $M+H^+$ ]. The mass corresponds to the sum of the masses of the demetallated protoporphyrin IX-dimethyl ester ( $M_r = 590.3$ ) and artemisinin fragment **5** after hydrolysis of the oxygen–iron bond ( $M_r = 283.2$ ) minus one mass unit, which leads to covalent adducts **6a**, **6b**, and **6c** (Scheme 1b, calculated mass: 872.5). This result confirmed that no extensive degradation occurred during the demetallation step.

To elucidate the substitution positions by the artemisinin fragment, different NMR sequences were used, including COSY, NOESY, and 1D-NOE selective excitation. The resonance of the NH protons was detected at  $\delta = -2.79$ , strongly deshielded with respect to protoporphyrin IX-dimethyl ester ( $\delta = -3.94$ ). This result was consistent with a direct substitution on the macrocycle, which leads to a lowering of the ring current effect. The main *meso* protons were detected as nine singlets at  $\delta = 9.8$ –10.3, which suggests the presence of three different isomers that result from the substitution of three different *meso* positions of **6** (Figure 1a; the broad singlet at  $\delta = 10.13$  is due to an impurity and does not belong to the heme-artemisinin adducts. This was confirmed by <sup>1</sup>H–<sup>13</sup>C correlation: this peak was not connected to a carbon atom with a signal at  $\delta = 95$ –100, the expected region for *meso*-carbon resonances). Thus, the NMR data confirm that three regioisomers were formed. The vinylic H<sub>c</sub> protons gave rise to signals at  $\delta = 8.05$ –8.30 (2H, six doublets of doublets, Figure 1b), and H<sub>a</sub> and H<sub>b</sub> resulted in a complex pattern at  $\delta = 5.94$ –6.39 (4H, 12 multiplets) with integration values consistent with those of other porphyrin protons, namely CH<sub>2</sub> units ( $\delta = 4.37$ , 4H;  $\delta = 3.25$ , 4H) and CH<sub>3</sub> units ( $\delta = 3.5$ –3.7, 18H). This result ruled out the hypothesis of substitution of a vinylic position by the artemisinin fragment. All the significant protons of the artemisinin moiety were detected and showed the correct integration: the doublets for the methyl groups at C6 and C9 were detected at  $\delta = 0.92$  and 1.22, respectively; H12 and the acetate protons were detected as singlets at  $\delta = 5.60$  (compared to 5.85 in artemisinin) and  $\delta = 1.59$ , respectively, and H9 gave rise to a multiplet at  $\delta \approx 3.21$  (compared to ca. 3.33 in artemisinin). These signals confirmed that the complete structure of artemisinin was retained and that no modification occurred on the lactone ring. Furthermore, the C4 methylene protons appeared as two broad signals at  $\delta = 5.15$  and 5.45, as expected for a methylene substituent at the *meso* positions of

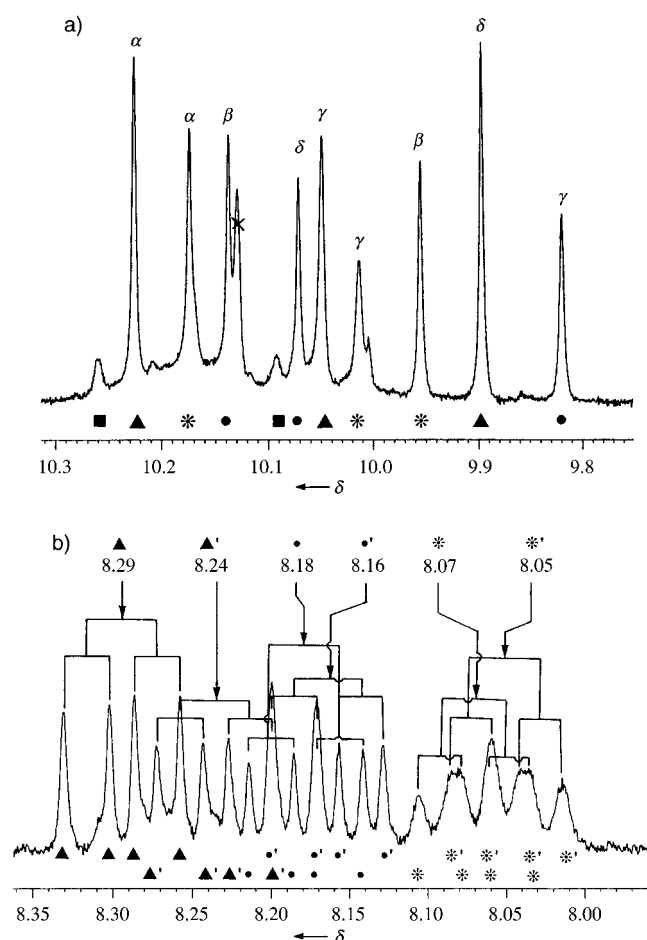


Figure 1.  $^1\text{H}$  NMR spectrum of the artemisinin-heme adducts: a) region of *meso*-H resonances, which indicate substitution on the  $\alpha$ -carbon **6a** (●),  $\beta$ -carbon **6b** (▲),  $\delta$ -carbon **6c** (\*). A minor covalent adduct, which corresponds to the substitution of  $\gamma$ -carbons, was also detected (■); b) region of  $\text{H}_c$  protons for adducts **6a** (●,  $\alpha$ -substitution), **6b** (▲,  $\beta$ -substitution), and **6c** (\*,  $\delta$ -substitution).

protoporphyrin,<sup>[12]</sup> and NOE interactions were observed between the C4-methylene and the vinyl  $\text{H}_c$ , thus confirming the existence of a covalent coupling between an artemisinin residue and the *meso* carbon atoms of heme.

The substituted *meso* positions were then identified by NMR spectroscopy. 1D-NOE selective irradiation of the propionate methylene protons ( $\delta = 4.37$ ) allowed the identification of three different  $\gamma$ -protons. Two different  $\delta$ -protons were characterized from their NOE interactions with two methyl groups each. The sequential correlations  $\delta\text{-H} \rightarrow \text{H}_3\text{C-C2}' \rightarrow \text{H}_a\text{-C}=\text{C-C3}' \rightarrow \text{H}_c\text{-C-C3}' \rightarrow \alpha\text{-H}$  on one hand, and  $\gamma\text{-H} \rightarrow \text{H}_2\text{C-C13}' \rightarrow \text{H}_3\text{C-C12}' \rightarrow \beta\text{-H}$  on the other hand, allowed the identification of two  $\alpha$ - and two  $\beta$ -protons (Figure 1 a). We thus confirmed that the three main covalent adducts resulted from the non-regioselective substitution of artemisinin at the  $\alpha$ - (●),  $\beta$ - (▲), and  $\delta$ -carbons (\*) (28:39:33, respectively). A minor covalent adduct which results from the substitution of  $\gamma$ -carbons was also detected (■; less than 7–12 % of the total amount of adducts).

In control experiments, we checked that  $[\text{Fe}^{\text{III}}(\text{ppix-dme})\text{Cl}]$  (**3**) did not react with artemisinin in the absence of hydroquinone derivative, and that the porphyrin macrocycle

was not modified by 2,3-dimethylhydroquinone in the absence of artemisinin. Furthermore, when *tert*-butylhydroquinone or thiobenzyl alcohol were used instead of 2,3-dimethylhydroquinone, the reaction occurred in the same way and afforded the same adducts, which confirms that the formation of adducts did not depend on the reducing agent used, provided that it was able to reduce the iron(III) center of the heme derivative to the ferrous state.

The reaction of artemether with  $[\text{Fe}^{\text{II}}(\text{ppix-dme})]$  under the same conditions used for artemisinin afforded metallated adducts that showed a mass increment of 16 uma with respect to the mass spectrum of metallated covalent adducts heme-artemisinin, consistent with the difference of 16 between the molecular weight of artemisinin and that of artemether. This indicates that heme was also alkylated by artemether **4**. Unfortunately, the demetallation procedure used for artemisinin can not be used in this case, because of the lability of the B ring of artemether under strongly acidic conditions;<sup>[9]</sup> full assignment by NMR was thus impossible.

The reductive activation of artemisinin (or artemether) by heme is able to produce covalent heme-artemisinin adducts in high yields under very mild conditions by the alkylation of the *meso* positions. The reduced heme involved in the two-step generation of the C-centered alkylating radical of artemisinin can be produced by the large excess of reducing agents present in erythrocytes (e.g. 1 mM of glutathione). The carbon-centered radicals derived from antimalarial trioxanes by activation with the reduced heme are probably able to alkylate the release heme at pharmacological concentrations of the drug,<sup>[6]</sup> which lead to the death of the parasite through the accumulation of non-polymerizable redox-active heme adducts. In addition, the C4 radical of artemisinin or artemether might escape from reduced heme and be able to alkylate one (or several) protein(s) involved in the degradation of hemoglobin or the polymerization of heme.<sup>[13]</sup>

## Experimental Section

Iron(III) protoporphyrin-IX dimethylester chloride:  $[\text{Fe}^{\text{III}}(\text{ppix-dme})\text{Cl}]$  (**3**) was prepared from  $[\text{Fe}^{\text{III}}(\text{ppix})\text{Cl}]$  (hemin) according to a published procedure.<sup>[11]</sup> MS (DCI/ $\text{NH}_3^+$ ):  $m/z$  645  $[\text{M}+\text{H}^+]$  for  $[\text{Fe}^{\text{II}}(\text{ppix-dme})]$  (the loss of the axial ligand and the reduction of the metal center are often observed during MS analyses of metalloporphyrins).<sup>[14]</sup>

Covalent adducts **6**:  $[\text{Fe}^{\text{III}}(\text{ppix-dme})\text{Cl}]$  (**3**, 40 mg, 59  $\mu\text{mol}$ ) and **1** (50 mg, 177  $\mu\text{mol}$ , 3 equiv) were dissolved in dichloromethane (4 mL). This solution was degassed and kept under an argon atmosphere. 2,3-Dimethylhydroquinone (82 mg, 590  $\mu\text{mol}$ , 10 equiv) was then added as a solid, and the solution was stirred at room temperature under argon. When the conversion of hemin was complete, an aliquot was withdrawn for MS analysis of the crude metallated adducts (MS (ESI $^+$ ):  $m/z$  (relative intensity): 926.5 (55)  $[\text{M}^+]$ , 866.5 (100)  $[\text{M}^+ - \text{CH}_3\text{COOH}]$ ; MS (DCI/ $\text{NH}_3^+$ ):  $m/z$ : 884  $[\text{M}+\text{NH}_4^+ - \text{CH}_3\text{COOH}]$ , 867  $[\text{M}+\text{H}^+ - \text{CH}_3\text{COOH}]$ ). Degassed acetic acid (30 mL) was then added under argon, followed by a suspension of  $\text{Fe}^{\text{II}}\text{SO}_4 \cdot 1.5\text{H}_2\text{O}$  (180 mg, 1.0 mmol, 17 equiv) in 37 wt % hydrochloric acid (1.2 mL) and the mixture was stirred at room temperature. The demetallation of hemin derivatives was complete within few minutes. Dichloromethane (30 mL) was then added under air, and the organic layer was washed with aqueous sodium acetate (1M, 4  $\times$  50 mL). The dichloromethane solution was dried over sodium sulfate, filtered, and evaporated to dryness. The adducts **6a**, **6b** and **6c** were recovered as a mixture after chromatography of the crude product over a column of silica gel 60, with hexane/dichloromethane/ethyl acetate 40:25:35, v/v/v as eluent. UV/Vis ( $\text{CH}_2\text{Cl}_2$ ):  $\lambda_{\text{nm}}$  (relative intensity): 414 (100), 512 (10), 582<sub>sh</sub> (5), 540

(6); MS (ESI<sup>+</sup>):  $m/z$  (relative intensity): 873.5 (10) [ $M+H^+$ ], 813.5 (100) [ $M+H^+ - CH_3COOH$ ]. MS (DCI/NH<sub>3</sub><sup>+</sup>):  $m/z$ : (relative intensity) 873 (2) [ $M+H^+$ ], 816 (6), 815 (20), 814 (52), 813 (100) [ $M+H^+ - CH_3COOH$ ], 812 (4); <sup>1</sup>H NMR (400.13 MHz, CDCl<sub>3</sub>, for clarity, the signals of the porphyrin moiety are described first, and then those of the artemisinin fragment):  $\delta$  = 10.23, 10.17, 10.14, 10.07, 10.05, 10.01, 9.96, 9.90, 9.82 (9  $\times$  s, 3 H, *meso*-H), 8.29, 8.24, 8.18, 8.16, 8.05, 8.07 (6  $\times$  m, 2 H, H<sub>2</sub>), 6.39, 6.30, 6.31, 6.20, 6.16, 5.94 (4 H, H<sub>a</sub> and H<sub>b</sub>), 4.37 (m, 4 H, H<sub>2</sub>C-C13' and H<sub>2</sub>C-C17'), 3.75–3.57 (18 H, H<sub>3</sub>C-C2', H<sub>3</sub>C-C7', H<sub>3</sub>C-C12', H<sub>3</sub>C-C18', and COOCH<sub>3</sub>), 3.25 (m, 4 H, H<sub>2</sub>CCOOCH<sub>3</sub>), –2.79 (2 H, NH), 5.45 and 5.15 (2  $\times$  m, 2  $\times$  H, H<sub>2</sub>C4), 2.07, 1.77, 1.56 (H<sub>2</sub>C5), 1.11 and 0.58 (H5a), 1.28 (m, 1 H, H6), 0.92 (d, 3 H, <sup>3</sup>J = 6 Hz, H<sub>3</sub>C-C6), 1.98 and 1.51 (H<sub>2</sub>C7), 1.93 and 0.98 (H<sub>2</sub>C8), 2.06 (H8a), 3.21 (m, 1 H, H9), 1.22 (d, 3 H, <sup>3</sup>J = 7 Hz, H<sub>3</sub>C-C9), 5.60 (s, 1 H, H12), 1.59 (s, 3 H, H<sub>3</sub>CCOO-C12), 1.53 (HO-C12a).

Analytical HPLC conditions: column: C8 on Lichrosorb 10  $\mu$ m (Interchrom, France); eluent A: 0.1 vol% aqueous trifluoroacetic acid, eluent B: CH<sub>3</sub>CN; gradient program: linear from 40% to 70% of eluent B for 50 min, then linear from 70% to 100% of B for the following 15 min, 1 mL min<sup>–1</sup>; products were detected at  $\lambda$  = 420 nm to follow the modifications of the porphyrin chromophore. To monitor the reaction, aliquots (50  $\mu$ L) were evaporated to dryness, dissolved in a mixture (1 mL, 1:1, v/v) of acetonitrile and aqueous trifluoroacetic acid (0.1 vol%), and analyzed (injected volume: 100  $\mu$ L). After 20–30 min of reaction time, the conversion of starting hemin (retention time = 26.6 min) was 85–90%. Two broad peaks of modified hemin derivatives were detected (retention time = 32.3, 33.1 min, respectively; ESI-MS:  $m/z$ : 926.5 [ $M^+$ ] for this mixture and for each of the two broad peaks recovered after semi-preparative HPLC.

Received: January 17, 2001 [Z16443]

- [1] N. J. White, F. Nosten, S. Looareesuwan, W. M. Watkins, K. Marsh, R. W. Snow, G. Kokwaro, J. Ouma, T. T. Hien, M. E. Molyneux, T. E. Traylor, C. I. Newbold, T. K. Ruebush, M. Danis, B. M. Greenwood, R. M. Anderson, P. Olliaro, *Lancet* **1999**, 353, 1965–1967.
- [2] S. Pagola, P. W. Stephens, D. S. Bohle, A. D. Kosar, S. K. Madsen, *Nature* **2000**, 404, 307–310.
- [3] S. R. Meshnick, T. E. Taylor, S. Kamchonwongpaisan, *Microbiol. Rev.* **1996**, 60, 301–315.
- [4] J. N. Cumming, P. Ploypradith, G. H. Posner, *Adv. Pharmacol.* **1997**, 37, 253–297.
- [5] A. Robert, B. Meunier, *Chem. Soc. Rev.* **1998**, 27, 273–279.
- [6] W. Asawamahaskda, I. Ittarat, Y.-M. Pu, H. Ziffer, S. R. Meshnick, *Antimicrob. Agents Chemother.* **1994**, 38, 1854–1858.
- [7] Y.-L. Hong, Y.-Z. Yang, S. R. Meshnick, *Mol. Biochem. Parasitol.* **1994**, 63, 121–128.
- [8] A. Robert, B. Meunier, *J. Am. Chem. Soc.* **1997**, 119, 5968–5969.
- [9] A. Robert, B. Meunier, *Chem. Eur. J.* **1998**, 4, 1287–1296.
- [10] G. H. Posner, C. H. Oh, D. Wang, L. Gerena, W. K. Milhous, S. R. Meshnick, W. Asawamahaskda, *J. Med. Chem.* **1994**, 37, 1256–1258.
- [11] J.-H. Fuhrhop, K. M. Smith in *Porphyrins and Metalloporphyrins* (Ed.: K. M. Smith), Elsevier, Amsterdam, **1975**, pp. 757–869.
- [12] H. Scheer, J. J. Katz in *Porphyrins and Metalloporphyrins* (Ed.: K. M. Smith), Elsevier, Amsterdam, **1975**, pp. 399–524.
- [13] A. V. Pandey, B. L. Tekwani, R. L. Singh, V. S. Chauhan, *J. Biol. Chem.* **1999**, 274, 19383–19388.
- [14] P. Bigey, S. Frau, C. Loup, C. Claparols, J. Bernadou, B. Meunier, *Bull. Soc. Chim. Fr.* **1996**, 133, 679–689.

## Assembly of Ni<sub>7</sub> and Ni<sub>21</sub> Molecular Clusters by Using Citric Acid\*\*

Mark Murrie, Helen Stoeckli-Evans, and Hans U. Güdel\*

Exploration of the middle ground between simple molecular species and infinite arrays has led to the discovery of novel, nanoscale materials in the field of molecular magnetism. Single Molecule Magnets (SMM)<sup>[1]</sup> offer the possibility of information storage at the molecular level, and have provided the first examples in which novel phenomena such as quantum-mechanical tunneling of magnetization can be observed.<sup>[2]</sup> It is now understood that a large spin ground state (S) and a negative axial anisotropy (D) are a prerequisite.

However, there is a perceived need to develop synthetic approaches to larger, more complex molecules to establish further the relationship between structure and molecular properties. By utilizing simple organic ligands, such as carboxylates, it has been possible to isolate clusters containing up to 24 transition metal ions.<sup>[3]</sup> The use of more complex ligands such as polycarboxylates<sup>[4]</sup> or polyalcohols,<sup>[5]</sup> has been more limited. Polydentate ligands should produce new cluster topologies by virtue of their coordinative flexibility.

We have chosen to investigate the proligand citric acid (HOC(CO<sub>2</sub>H)(CH<sub>2</sub>CO<sub>2</sub>H)<sub>2</sub>; H<sub>4</sub>cit) which has been little employed in cluster synthesis; only two high nuclearity (N  $\geq$  6) transition metal citrate complexes are structurally characterized.<sup>[6]</sup> Nevertheless, we have found that citrate displays a rich solution chemistry with Ni<sup>II</sup> units and herein report our first success in isolation of two new citrate clusters containing seven and an unprecedented 21 Ni<sup>II</sup> ions, respectively.

The reaction of Ni<sup>II</sup> with citrate in basic aqueous solution in the presence of Na<sup>+</sup> and NMe<sub>4</sub><sup>+</sup> ions, followed by the addition of ethanol as cosolvent gives the {Ni<sub>7</sub>} cluster **1** (see Experimental Section). The high solubility of such species in aqueous solution makes crystallization by slow evaporation difficult, as previously noted.<sup>[6a]</sup> We have addressed this problem by adjusting solvent polarity to effect crystallization, thus removing the need for crystallization from highly concentrated, and often viscous solutions. The single crystal X-ray structure of **1** (Figure 1) shows a cluster containing two {Ni<sub>3</sub>} trimers related by a pseudo two-fold axis passing through the central Ni (Ni4).<sup>[7]</sup> The coordination sites at the nickel centers are occupied by the oxygen atoms from the six citrate ligands, apart from a site on both Ni3 and Ni5, which is filled

[\*] Prof. Dr. H. U. Güdel, Dr. M. Murrie  
 Departement für Chemie und Biochemie  
 Universität Bern  
 Freiestrasse 3, 3000 Bern 9 (Switzerland)  
 Fax: (+41) 31-631-4399  
 E-mail: hans-ulrich.guedel@iac.unibe.ch  
 Prof. Dr. H. Stoeckli-Evans  
 Institut de Chimie  
 Université de Neuchâtel  
 Avenue de Bellevaux 51, 2000 Neuchâtel (Switzerland)

[\*\*] This work was supported by the Swiss National Science Foundation.